THE JOURNAL OF CHEMICAL PHYSICS VOLUME 16, NUMBER 4 APRIL, 1948

Nuclear Resonance Absorption in Hydrated Crystals: Fine Structure of the Proton Line

G. E. PAKE*
Lyman Laboratory of Physics, Harvard University, Cambridge, Massachusetts
(Received December 2, 1947)

Fine structure has been observed in the nuclear paramagnetic resonance absorption line for protons in crystalline hydrates. The magnetic field of 6820 gauss was provided by a permanent magnet, the inherent stability of which facilitated detailed study of line shape. Measurements on a single crystal of $CaSO_4 \cdot 2H_2O$ show a splitting into four component lines with maximum separation varying from zero to 22 gauss, depending upon the direction of the externally applied magnetic field in the crystal. Both the number of component lines and the dependence of their spacing on field direction are calculated by treating the magnetic dipole-dipole interaction as a perturbation of the proton two-spin system within the water molecule; the effect of the more distant protons, neglected in this calculation, gives a finite width to the component lines. Variation of the splitting with field direction determines the orientation of the line joining protons in the water molecule, which is found to be consistent with positions ascribed to hydrogen nuclei in the lattice through simple considerations of chemical bonding. The distance between protons in the water molecule is measured by the splitting to be 1.58A for $CaSO_4 \cdot 2H_2O$; if one assumes an H−O−H bond angle of 108°, the O−H distance is 0.98A. Powdered hydrates show a characteristic fine structure arising from isotropic distribution in solid angle of single crystal granules. This type of fine structure determines the proton-proton distance somewhat less accurately than does the single crystal experiment.

1. INTRODUCTION

THE width and shape of a nuclear resonance absorption line are profoundly influenced by the magnetic environment of the absorbing nuclei. In addition to the externally applied field $\mathbf{H}_0$, a local field produced by neighboring nuclear and in some instances electronic magnetic moments contributes to this environment. In gases, liquids, and certain solids, relative motion between nuclei causes the field at a given nucleus to fluctuate rapidly about the value $\mathbf{H}_0$, and the local fields tend to average out. Indeed, the resonance in non-paramagnetic substances of this type occurs within such a narrow range of field values[1] that inhomogeneities in the externally applied field often determine the measured line width[2] and shape. The atomic nuclei in crystalline solids, however, usually occupy definite lattice positions to which they are bound by crystalline fields. To the extent to which these nuclei are rigidly fixed, the interaction of static magnetic dipoles may be expected to determine line widths and line shapes, at least for those nuclei ($I=\frac{1}{2}$) which possess no electric quadrupole moment.

Since the interaction between magnetic dipoles falls off as the inverse cube of the separating distance, nuclear moments in certain crystals, e.g., protons in water molecules of hydration, may possibly occur in pairs the members of which are so closely spaced that each nucleus finds itself predominately in the local field of its partner. Classically we should then expect each nuclear dipole to produce at its partner a field of several gauss, the component of which along the $\mathbf{H}_0$ field of several thousand gauss[3] will alter somewhat the effective large field. In fact, if θ is the angle between $\mathbf{H}_0$, taken in the z direction, and the line joining the two interacting nuclei, this local field component varies as $3\cos^2\theta-1$ and space quantization of the nuclear spin in the $\mathbf{H}_0$ field should produce nuclear resonance fine structure governed by this angular factor. In particular, for spin $\frac{1}{2}$, we may naively write the magnitude of the effective field at one nucleus of the pair as

$$H_{eff}=H_0\pm\alpha(3\cos^2\theta-1), \qquad (1)$$

where the $\pm$ sign attempts to account for the two possible values of the z component of the partner's magnetic moment, and α is an inter-

* Predoctoral Fellow of the National Research Council.
[1] N. Bloembergen, R. V. Pound, and E. M. Purcell, Phys. Rev. 71, 466 (1947).
[2] Unless otherwise specified, "line width" means throughout this paper one-half the width of a simple bell-shaped resonance curve at half-maximum intensity.
[3] Although in a strict sense we require the magnetic induction B or even the microscopic field, the proper unit for either of which is the gauss, we conform to widespread usage by referring to a magnetic field H in gauss. This should cause no confusion.

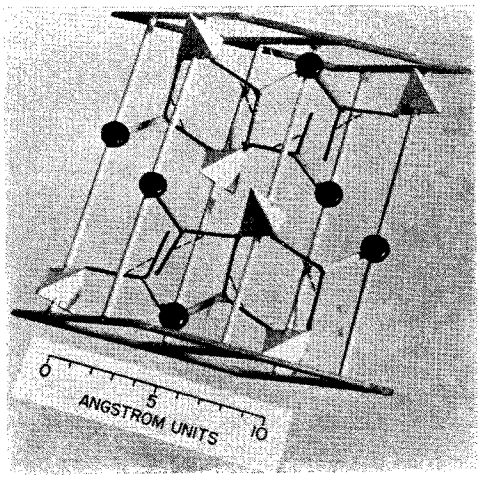

FIG. 1. Model of the gypsum unit cell. Spheres are Ca^{++}, tetrahedra are SO_4^{--}, and black V structures have vertices at water oxygens, each arm being an O—H···O bond. The dashed lines indicate the direction of the proton-proton lines in water molecules as verified by the experiment.

action field parameter to be fixed by a more careful analysis (Section 5). Thus the naive picture predicts a pair of nuclear resonance lines symmetrically disposed about the field value at which a simple resonance line would occur. This note discusses such fine structure found in the proton resonance absorption lines of certain hydrated crystalline solids. An interesting experimental result is the measurement of the distance between hydrogen nuclei in the water molecules of hydration, as well as the determination of the orientation of the line connecting the proton pair in the molecule.

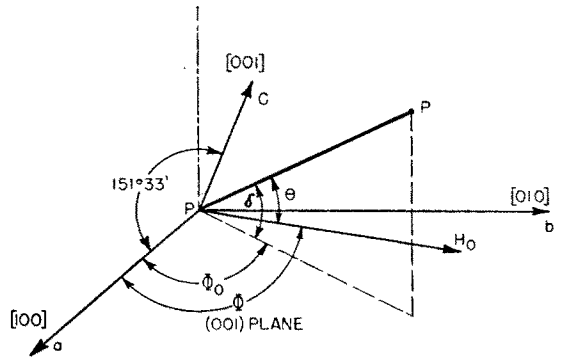

FIG. 2. Diagram defining various angles relating $\mathbf{H}_0$ direction to crystal axes and to the proton-proton line $p-p$ in a water molecule of the gypsum lattice.

2. THE CRYSTAL STRUCTURE OF GYPSUM

Gypsum, $CaSO_4 \cdot 2H_2O$, contains no paramagnetic ions and is a relatively simple hydrate in that the only nuclei with non-vanishing spin, and therefore with a magnetic moment, are the protons in the water molecules. Large single crystals exist in nature, and the structure is known through the careful investigation of Wooster.[4] The unit cell contains four molecules; its a or [100] edge is 10.47A, the b or [010] edge is 15.15A, and the c or [001] edge is 6.51A. Axes a and b are perpendicular, as are c and b, but the angle between positive a and c directions is 151° 33′. The crystal has a perfect cleavage parallel to the (010) plane and a fibrous cleavage parallel to the $(\bar{1}11)$ plane.

Figure 1 shows a model of the unit cell constructed from Wooster's results. The black spheres are Ca^{++} ions, the tetrahedra are SO_4^{--} ions, and the black V-shaped structures have their vertices at oxygen atoms of water molecules. Since x-ray methods do not locate hydrogen nuclei, the exact position of the protons is not known. However, it is expected from simple considerations of chemical binding that the hydrogen nuclei form two O—H···O bonds, the large angle between which is approximately bisected by a $Ca^{++}-O_{water}$ bond.[5] Each arm of a V structure represents such an O—H···O bond; the H—O—H bond angle in the crystal on this assumption is 108°, very little different from the 104° 31′ value in the gas as determined from analysis of vibration spectra.[6] If the O—H distance for both protons of the water molecule is the same, the line joining protons (hereafter referred to as the p–p line) and the line joining the two sulfate oxygens are parallel. Calculation from Wooster's data reveals that there are two permitted p–p directions in the gypsum crystal, four of the eight water molecules in the unit cell belonging to each direction. The two groups are easily distinguished in Fig. 1.

In one experiment to be described, the crystal was so cut that the $\mathbf{H}_0$ field could take any direction in the (001) plane through rotation of

[4] W. A. Wooster, Zeits. f. Krist. **94**, 375 (1936).
[5] A. F. Wells, *Structural Inorganic Chemistry* (Oxford University Press, New York, 1945), p. 370; Wooster, see reference 4, pp. 387 and 391.
[6] B. T. Darling and D. M. Dennison, Phys. Rev. **57**, 128 (1940).

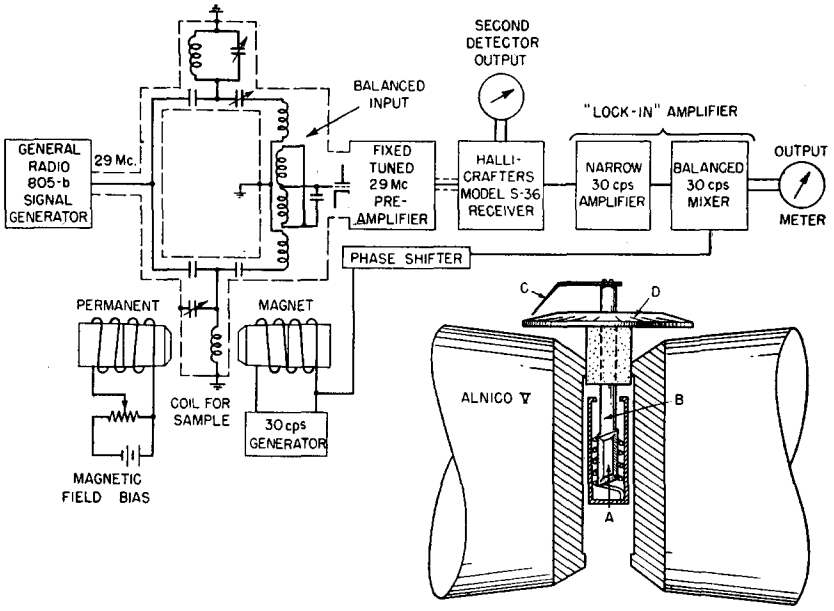

FIG. 3. Block diagram of apparatus and section through magnet gap. Pole face diameter is 4 in. and the gap is 0.780 in. in the region occupied by the sample. The pole face rim is raised 0.015 in. to improve radial homogeneity of the field.

the crystal in the field. Inasmuch as the p–p lines do not lie in this plane, the angle θ occurring in Eq. (2) must be related to the angle of inclination δ of these lines with the plane. From Fig. 2, where Φ_0 is the angle between [100] and the projection of p–p on the a–b or (001) plane, Φ the angle between [100] and $\mathbf{H}_0$, and δ the angle between p–p and its projection, it follows that

$$\cos\theta = \cos\delta \cos(\Phi - \Phi_0). \quad (2)$$

Calculations prove the second permitted p–p direction to be the reflection of the first in the (010) plane, and we expect, in general, to observe two pairs of lines at applied field values given by the two relations

$$H_0 = H^* \pm \alpha[3\cos^2\delta \cos^2(\Phi - \Phi_0) - 1], \quad (3a)$$

$$H_0 = H^* \pm \alpha[3\cos^2\delta \cos^2(\Phi + \Phi_0) - 1], \quad (3b)$$

where $H^* = h\nu/2\mu$ is the resonance field for magnetic moment μ and an applied radiofrequency ν, and where Φ_0 is calculated to be 54° 34′ from Wooster's data.

3. EXPERIMENTAL ARRANGEMENT

The experiments were performed at room temperature using the modulation method developed by Pound, Purcell, and Torrey.[7] A schematic diagram of the apparatus is shown in Fig. 3. Each pole of the permanent magnet consists of two Alnico V castings obtained from the Indiana Steel Company, one 6 in. in diameter and 6 in. long, and the other tapered from 6 in. to 5 in. in diameter in the same length. The smaller ends of the tapered castings are fitted with $\frac{1}{2}$-in. thick iron pole caps. The value of the magnetic field in the portion of the gap occupied by the r-f coil is measured by the frequency of the proton resonance, 28.981 mc, as 6816 gauss. Continuous and reversible variation of $\mathbf{H}_0$ from about 22 gauss below this value to 45 gauss above is accomplished by passing from -0.50 to $+1.0$ ampere through one of the two coils originally used to magnetize the Alnico. Current values appreciably outside this range are likely to affect the magnetization of the Alnico, i.e., produce changes in the value of the field at zero biasing current. Throughout the course of the experiments here reported, excessive biasing currents were avoided, and the reproducibility of the proton resonance at relatively fixed signal generator frequency sets a conservative upper limit of perhaps 2 gauss for magnetic field drift over a ten month operating period; no measurable change has been detected during an operating day. This freedom from stabilization problems, in addition to the fact that its field is always "set" at the resonance value once the proper

[7] R. V. Pound, E. M. Purcell, and H. C. Torrey, Phys. Rev. 69, 681 (1946).

radiofrequency circuit is available, especially adapts the permanent magnet to detailed line structure studies, which may be extended with ease to many different substances containing the nucleus under investigation.

By means of the narrow proton resonance in a liquid sample and a General Radio 620-A hetrodyne frequency meter, the variation of $\mathbf{H}_0$ with direct current was measured as 44.0 gauss per ampere, linear within 3 percent over the range from -15 to $+25$ gauss in which all measurements to be discussed were made. The width of liquid sample resonances in this magnet is about 0.2 gauss; such inhomogeneity is not prohibitive in the study of the broad lines occurring in solids.

The radiofrequency coil into which samples are inserted is $\frac{3}{8}$-in. inside diameter and $\frac{5}{8}$ in. long. Two gypsum crystals about $\frac{5}{16}$ in. in diameter and $\frac{3}{4}$ in. long were sawed from single crystals kindly provided by Professor C. S. Hurlbut of the Harvard Department of Mineralogy and Petrography. Each crystal (A in Fig. 3) has its cylinder axis normal to (001) and is cemented, with its axis along that of the mounting rod (B), to the end of a Teflon rod (du Pont fluorine-substituted poly-ethylene). Teflon gives no detectable proton signal, and a background line could only arise from the small quantity of cement, which subsequent experiments showed to be undetectable. The mounting rod is fitted with a pointer (C) movable over a circular scale (D), making possible angle measurements probably accurate to within half a degree. Powder samples are packed into $\frac{3}{8}$-in. diameter soft glass test tubes which may be inserted into the coil.

Measurement procedure begins with balancing the transmitted power output to a level about 50 db below the power level in either arm of the bridge, which is excited at 29.0 mc by a General Radio 805-b signal generator operating at about 0.15 output volts. The unbalanced signal results from comparison of two signals in phase but slightly different in amplitude, a condition necessary[8] for the measurement of absorption instead of dispersion, i.e., the imaginary instead of the real part of the nuclear susceptibility. Once steady balance is attained, the nuclear resonance line is mapped out point by point for successive values of $\mathbf{H}_0$. Inasmuch as the magnetic field is modulated at 30 cycles per second, the narrow

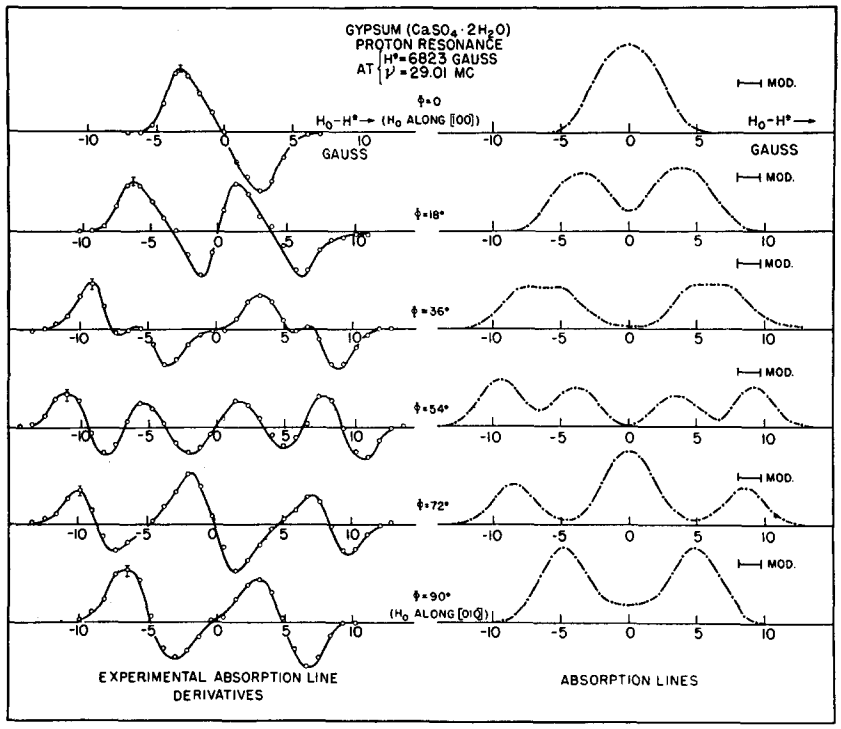

FIG. 4. Representative experimental absorption curve derivatives and their integrals for various directions of the externally applied magnetic field $\mathbf{H}_0$ in the (001) plane of a gypsum single crystal. The ordinates are measured in arbitrary units, and the region within which noise fluctuations occurred is indicated at the first maximum of each derivative. Peak-to-peak modulation sweep, indicated by the horizontal line near each integral, was 1.5 gauss for all curves.

[8] N. Bloembergen, R. V. Pound, and E. M. Purcell, Phys. Rev. 73, 679 (1948).

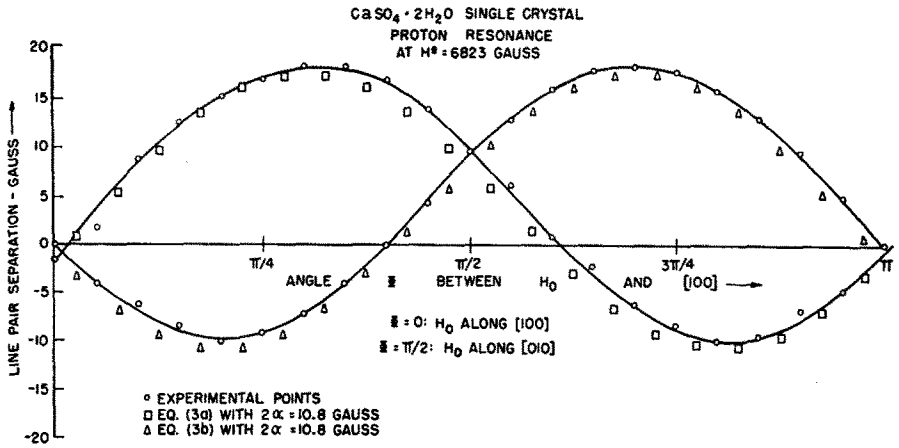

FIG. 5. Line pair separation as a function of the angle Φ between $\mathbf{H}_0$ and [100]. Because two directions exist for proton-proton lines in a gypsum single crystal, there are two similar curves differing in phase.

30-cycle amplifier and balanced mixer (or "lock-in" amplifier) measures the derivative of the nuclear susceptibility provided the total sweep of the modulating field is not too large in comparison with the width of the line.[8] Superposed upon the derivative at any point is a small random fluctuation of the meter reading resulting from the 30-cycle component of the noise spectrum. Experimental curves are taken with as small modulation sweep as is consistent with a good signal-to-noise ratio on the "lock-in" meter. Measurements were made at low enough signal generator power to preclude saturation, and the radiofrequency field of 10^{-2} gauss contributes negligibly to the observed line width.

4. EXPERIMENTAL RESULTS

Single Crystals

Data for gypsum single crystals consist of absorption curve derivatives, recorded at 9° intervals, for values of Φ between 0° and 180°. Three such sets of data, all in good agreement, were recorded for two specimens cut from different single crystals. Figure 4 shows representative experimental curves and their integrals. Total modulation sweep was 1.5 gauss, indicated by the horizontal line near each integral curve, and the range within which noise fluctuations occurred is indicated at the first maximum of each experimental derivative curve. It should be borne in mind that the experimental uncertainty in the points is less than the region defined by the upper and lower bounds of noise fluctuation.

In general, the resonance is split into a fine structure consisting of four lines, two pairs each of which is symmetrically disposed about H^*. For $\Phi=0$, $\mathbf{H}_0$ parallel to [100], it happens that all four lines nearly coincide, giving rise to a single bell-shaped curve. At $\Phi=18°$, both pairs have nearly the same separation and two peaks arise, each of which has begun to split at $\Phi=36°$. At 54°, all four lines are evident, and so on. If the experimentally measured line pair separations are plotted against Φ, the curves of Fig. 5 are obtained; the finite width of the four component lines makes separation determinations somewhat less accurate in those instances where lines nearly coincide. Since we hope to find agreement with the angular factors in Eq. (3), the sign of the plotted separation is changed each time it passes through zero. The square points and the triangular points are those calculated from Eq. (3a) and Eq. (3b), respectively, with $2\alpha=10.8$ gauss. Inasmuch as the crystal specimens were cut with no great angular precision, the agreement between experimental and calculated curves with regard to angular dependence is satisfactory.

Single crystals of $Na_2SO_4 \cdot 10H_2O$ show marked dependence of line shape on field direction, but little is known of the detailed structure of the decahydrates and there appear to be so many permitted p–p directions that the fine structure is not easily interpreted. Other difficulties with this substance will be discussed in Section 7.

Powdered Hydrates

Figure 6 shows experimental absorption curves for powdered $CaSO_4 \cdot 2H_2O$ and $KF \cdot 2H_2O$. In

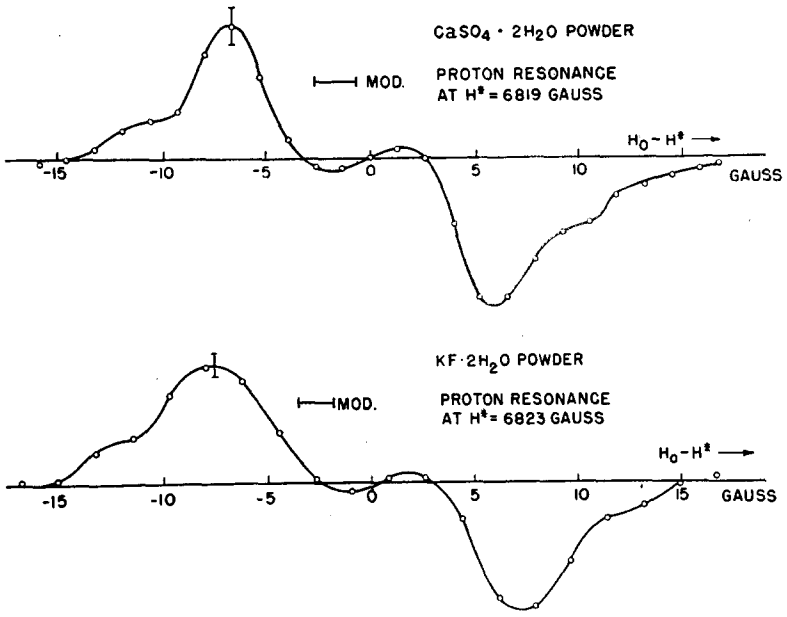

FIG. 6. Experimental derivatives of the proton absorption line in two powdered hydrates.

addition, $MgSO_4 \cdot 7H_2O$, $ZnSO_4 \cdot 7H_2O$, and $KAl(SO_4)_2 \cdot 12H_2O$ have quite similar absorption curves, the separation between minimum and maximum derivative values falling between 12.5 and 14.5 gauss for all five substances. All five derivatives indicate absorption lines with flat tops just resolved into two central maxima. In addition, very small humps tend to skirt either side of the flat-topped curve. In Section 6 we shall find a simple explanation of this shape in terms of the proton-proton interaction.

Powdered hydrates in which the line does not have structure of this type include not only paramagnetic salts but also borax, $Na_2B_4O_7 \cdot 10H_2O$, which has a simple curve with width of about 4.4 gauss. Experimental curves for $Na_2SO_4 \cdot 10H_2O$ have 14-gauss separation between derivative maximum and minimum, but the absorption curve has a more rounded central maximum.

5. CALCULATION OF LINE SHAPE FOR A SINGLE CRYSTAL AND COMPARISON WITH EXPERIMENT

We suppose that the resultant electronic magnetic moments vanish in the completed shells of the non-paramagnetic crystal ions. If the rigidly bound nuclei occur in close-spaced pairs such that each interacts in first approximation with its partner only, we may regard the crystal, magnetically at least, as a large number of independent nuclear moment pairs whose Zeeman levels are perturbed by the dipole-dipole interaction

$$V = \mu^2 r^{-3}(\boldsymbol{\sigma}_1 \cdot \boldsymbol{\sigma}_2 - 3\boldsymbol{\sigma}_1 \cdot \mathbf{r}_1 \boldsymbol{\sigma}_2 \cdot \mathbf{r}_1). \quad (4)$$

Here r is the distance between nuclei of the pair, $\mathbf{r}_1$ is a unit vector directed from one nucleus to the other, $(h/4\pi)\boldsymbol{\sigma}_k$ is the intrinsic angular momentum operator for spin $\frac{1}{2}$, and $\boldsymbol{\mu}_k = \mu\boldsymbol{\sigma}_k$ is the magnetic moment operator; for protons, $\mu = 2.7896$ nuclear magnetons.

The correct zero-order wave functions for the crystal are exceedingly complex ones involving the lattice and spin coordinates of all nuclei. However, our assumption of rigidly bound protons suppresses the multiplicative vibrational function, just as the assumption of "frozen-in" orbital magnetic moments facilitates treatment of paramagnetic relaxation in electron spin systems.[9] Because vibrational factors are neglected, the zero-order spin functions include both symmetric and antisymmetric representations. If the nuclear moments interact only within pairs, these are the functions for a two-spin system. To avoid degeneracy of the two $m=0$ levels, where m is the total magnetic quantum number of the two-spin system, we choose at the outset the triplet and singlet functions for the calcula-

[9] L. J. F. Broer, Physica **10**, 801 (1943).

tion of the matrix elements of V. Transitions from the triplets to the singlet are highly forbidden, and we need concern ourselves only with the diagonal elements for the triplet levels. Inspection of the identity

$$\begin{aligned}&\boldsymbol{\sigma}_1\cdot\boldsymbol{\sigma}_2-3\boldsymbol{\sigma}_1\cdot\mathbf{r}_1\boldsymbol{\sigma}_2\cdot\mathbf{r}_1\\&=\tfrac{1}{2}(3\cos^2\theta-1)(\boldsymbol{\sigma}_1\cdot\boldsymbol{\sigma}_2-3\sigma_{1z}\sigma_{2z})\\&-\tfrac{3}{4}(\sigma_{1x}+i\sigma_{1y})(\sigma_{2x}+i\sigma_{2y})\sin^2\theta e^{-2i\phi}\\&-\tfrac{3}{4}(\sigma_{1x}-i\sigma_{1y})(\sigma_{2x}-i\sigma_{2y})\sin^2\theta e^{2i\phi}\\&-\tfrac{3}{2}[\sigma_{2z}(\sigma_{1x}+i\sigma_y)+\sigma_{1z}(\sigma_{2x}+i\sigma_{2y})]\\&\qquad\times\sin\theta\cos\theta e^{-i\phi}\\&-\tfrac{3}{2}[\sigma_{2z}(\sigma_{1x}-i\sigma_{11y})+\sigma_{1z}(\sigma_{2x}-i\sigma_{2y})]\\&\qquad\times\sin\theta\cos\theta e^{i\phi},\end{aligned}\tag{5}$$

which is easily verified by expansion, yields the diagonal elements $(m|V|m)$ immediately. Since $\boldsymbol{\sigma}_1\cdot\boldsymbol{\sigma}_2=+1$ for triplets and only the first term of the right member contributes, it follows that

$$\begin{aligned}(-1|V|-1)&=-\mu^2r^{-3}(3\cos^2\theta-1),\\(0|V|0)&=2\mu^2r^{-3}(3\cos^2\theta-1),\\(1|V|1)&=-\mu^2r^{-3}(3\cos^2\theta-1).\end{aligned}\tag{6}$$

The unperturbed levels W_0^m and the perturbed levels W^m are shown diagrammatically in Fig. 7. The relative shifts are of the order of α/H_0, or less than 10^{-3} for the experiments reported here; clearly, the first-order correction suffices.

Resonance absorption occurs for the perturbed system when the following conditions obtain:

$$\begin{aligned}&m=+1\rightarrow m=0:\\&\qquad h\nu=2\mu H_0+3\mu^2r^{-3}(3\cos^2\theta-1),\\&m=0\rightarrow m=-1:\\&\qquad h\nu=2\mu H_0-3\mu^2r^{-3}(3\cos^2\theta-1).\end{aligned}\tag{7}$$

Substitution of $h\nu=2\mu H^*$ yields the resonance value for the external field as

$$H_0=H^*\pm\alpha(3\cos^2\theta-1),\tag{8}$$

with $\alpha=\frac{3}{2}\mu r^{-3}$. This equation locates a pair of fine structure lines for each existing direction θ in the sample. Since there are just two orientations of the p–p lines in the gypsum single crystal, we obtain the two pairs of lines which simple considerations of Sections 1 and 2 earlier led us to expect.

The calculated points fitted to the gypsum curve in Fig. 5 have $2\alpha=10.8$ gauss, from which the p–p distance is 1.58A. With the assumed bond angle of 108°, the O–H distance in the water molecule of crystallization would be 0.98A, a value not inconsistent with the interpretation of vibration frequencies in ice as corresponding to 0.99A when an O–H···O bond is formed.[10] It is perhaps well to emphasize that, had we not guessed the structure leading to the correct orientation of the p–p lines, curves such as those

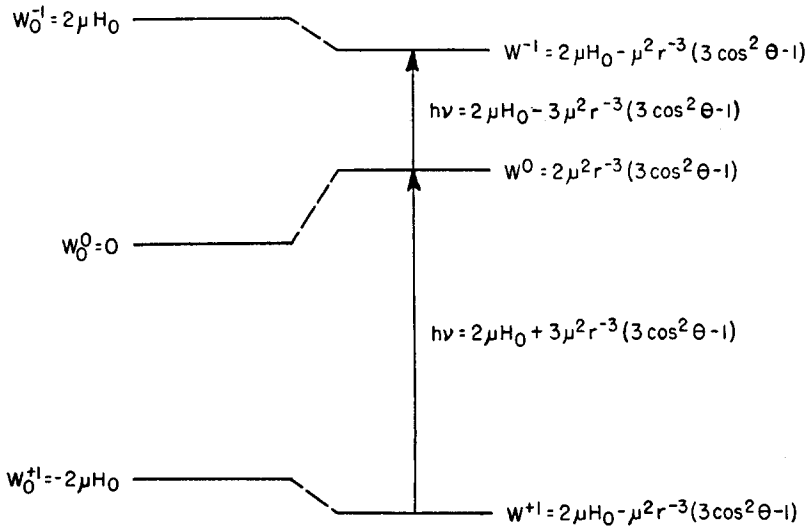

FIG. 7. Energy level diagram showing the effect of the perturbing dipole-dipole interaction on the ordinary Zeeman levels W_0^m of the two-proton system.

[10] P. C. Cross, J. Burnham, and P. A. Leighton, J. Am. Chem. Soc. 59, 1134 (1937); L. Pauling, *The Nature of the Chemical Bond* (Cornell University Press, Ithaca, New York, 1940), pp. 301–304.

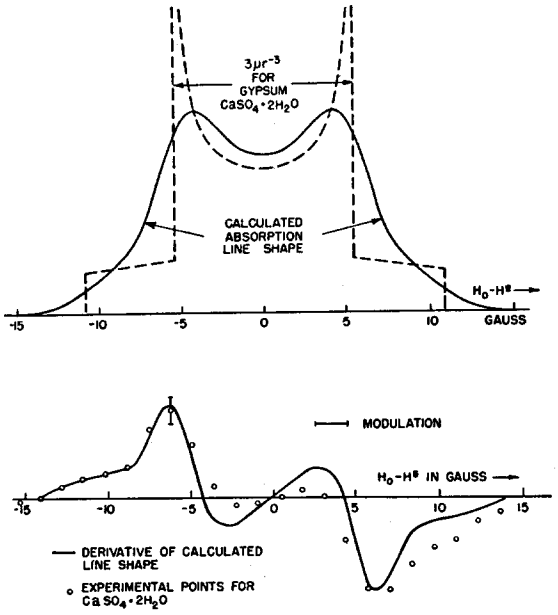

FIG. 8. The broken line in the upper curve shows the calculated distribution of component line centers for the proton resonance in powdered $CaSO_4 \cdot 2H_2O$. The continuous line on the same plot is the calculated line shape obtained by superposing gaussians of width 1.54 gauss according to this distribution function. The lower plot contains experimental points for powdered $CaSO_4 \cdot 2H_2O$, and a curve which is the derivative of the calculated line shape.

of Fig. 5 would have determined, to the accuracy with which the crystal was cut, the two permitted p–p directions in the lattice. The experiment measures directly only these directions and the p–p distance, not the O—H distance.

6. CALCULATION OF LINE SHAPE IN POWDERS AND COMPARISON WITH EXPERIMENT

The orientation of the small crystal granules comprising a powder may be described by an isotropic distribution-in-angle function. Such a distribution at once defines through Eq. (8) a distribution of resonance lines in the magnetic field. The probability for a transition governed by each sign in (8) is $\frac{1}{2}$ for purposes of intensity calculation, inasmuch as the Boltzmann factors of the triplet levels differ from unity by less than 10^{-5} at room temperature. Since $3\cos^2\theta - 1$ takes on all of its values in the range $\theta = 0$ to $\theta = \pi/2$, we write the angular distribution function over only this range of θ variation, and the number of transitions per unit time governed by the positive sign is

$$N_+ = \frac{N}{2}\int_0^1 d(\cos\theta) = \frac{N}{2}\int_{H^*-\alpha}^{H^*+2\alpha} p_+(H_0)dH_0, \quad (9)$$

where N is the total number of transitions per unit time and $p_+(H_0)dH_0$ is the probability that a transition for the positive sign in (8) occurs in a range dH_0. With Eq. (8), $d(\cos\theta)$ may be expressed in terms of H_0 and dH_0, yielding from (9)

$$N_+ = \frac{N}{2}\int_{-\alpha}^{2\alpha} (2\sqrt{3}\alpha)^{-1}\left(\frac{\Delta H}{\alpha}+1\right)^{-\frac{1}{2}} d(\Delta H), \quad (10)$$

where $\Delta H = H_0 - H^*$. Evidently changing the sign in Eq. (8) gives $p_+(-\Delta H) = p_-(\Delta H)$, and the resultant total distribution is

$$p(\Delta H) \sim \left(\frac{\Delta H}{\alpha}+1\right)^{-\frac{1}{2}} \text{ between } \Delta H = -\alpha \text{ and } \Delta H = +2\alpha$$
$$+\left(-\frac{\Delta H}{\alpha}+1\right)^{-\frac{1}{2}} \text{ between } \Delta H = -2\alpha \text{ and } \Delta H = +\alpha. \quad (11)$$

This function, with $\alpha = 5.4$ gauss as measured for the gypsum single crystal, is exhibited in Fig. 8 as the broken line. But just as Eq. (8) merely locates the center of each resonance line, so $p(H_0 - H^*)dH_0$ is the probability that the center of a fine structure component line occurs in dH_0, and the resultant absorption line for a powder is a superposition of bell-shaped curves of finite width, weighted by the probability that their centers fall in dH_0. If $f(H)$ is the resultant shape function, then

$$f(H) = \int_{-\infty}^{\infty} p(H_0 - H^*)S(H - H_0)dH_0, \quad (12)$$

where $S(H - H_0)$ is the shape of the component line. As taken from the outer lines of the curve for $\Phi = 72°$ in Fig. 4, the component line width produced by heretofore neglected next nearest neighbors and field inhomogeneities is 1.54 gauss. This is consistent with μr^{-3} calculated to be about 0.7 gauss for the next nearest proton, about 2.8A away, and with inhomogeneity-produced widths of 0.2 gauss.

The smooth curve in Fig. 8 is calculated from Eq. (12), using α for gypsum and a gaussian component line $S(H - H_0) = \exp[-(H - H_0)^2/$

$2\beta^2]$ with $\beta=1.54$ gauss. As might be expected, one observes slight variation with $\mathbf{H}_0$ direction in the width of component lines, for which the curve of Fig. 8 makes no allowance. The derivative of the calculated line is plotted in the lower portion of the figure, as are the experimental points for gypsum. Since the powder density is less than that of the single crystal, noise is more pronounced.

7. DISCUSSION

Although the detailed structure of $KF\cdot 2H_2O$ is not known, it is probable that $O-H\cdots F$ bonds exist,[11] in which event the fluorine nuclear moment is roughly as close to its neighboring proton as is the partner proton. Since the magnetic moment of F^{19} is 2.627 nuclear magnetons, the assumption of nearly isolated proton pairs seems highly questionable. Yet the fine structure is experimentally quite recognizable, consistent with a component line width of about 3 gauss.

To understand why the proton-proton interaction should predominate in this instance, it is instructive to consider the form which V in Eq. (4) would assume for two different nuclei of spin $\frac{1}{2}$, such as the proton and F^{19}. The portion of V with diagonal elements is then

$$V_{\text{disg}}=\tfrac{1}{2}(3\cos^2\theta-1)(\boldsymbol{\mu}_1\cdot\boldsymbol{\mu}_2-3\mu_{1z}\mu_{2z})r^{-3}.$$

If we write the operator $\boldsymbol{\mu}_1\cdot\boldsymbol{\mu}_2$ in the Heisenberg scheme, it becomes

$$(\boldsymbol{\mu}_1\cdot\boldsymbol{\mu}_2)_{\text{op}}=\mu_{1z}\mu_{2z}+\tfrac{1}{2}[(\mu_{1x}+i\mu_{1y})(\mu_{2x}-i\mu_{2y})e^{i(-\omega_{L1}+\omega_{L2})t}+(\mu_{1x}-i\mu_{1y})(\mu_{2x}+i\mu_{2y})e^{i(\omega_{L1}-\omega_{L2})t}],$$

where ω_{L1} and ω_{L2} are the respective Larmor frequencies of nuclei 1 and 2. If the nuclei are identical, the time drops out of the second term, which is then a secular perturbation contributing diagonal elements. But if ω_{L1} differs appreciably from ω_{L2}, the only secular part of $(\boldsymbol{\mu}_1\cdot\boldsymbol{\mu}_2)_{\text{op}}$ is given simply by $\mu_{1z}\mu_{2z}$, and the resonance lines are those of Eq. (8) with $\alpha_1=\mu_2 r^{-3}$ and $\alpha_2=\mu_1 r^{-3}$ for the respective resonances of nuclei 1 and 2. Thus for different Larmor frequencies, the result is identical with that which the naive picture would yield if we assumed the effective local field to arise from the static z component of the partner moment. One might say that the $\frac{3}{2}$ factor for identical nuclei is introduced by the coupling of the two precessing nuclei through the components of their magnetic fields which precess at the Larmor frequency; instead of making transitions individually, the coupled pair is flopped from one triplet level to the next. A like neighbor in a pair is thus $\frac{3}{2}$ as effective as an unlike neighbor in the same position would be.

Although the $\frac{3}{2}$-factor connecting the naive picture with reality can be shown to hold for three identical nuclei with spin $\frac{1}{2}$ on the vertices of an equilateral triangle normal to $\mathbf{H}_0$, it is not general for a many-spin system. As Professor Van Vleck has kindly pointed out to the author, this lack of generality is connected with the failure of the interaction between nuclei i and j to commute with that between i and k.[12]

In view of the "quantum-mechanically enhanced" effectiveness of like neighbors, it is surprising that the expected fine structure in borax, $Na_2B_4O_7\cdot 10H_2O$, gives way to a simple resonance line with a single maximum and a width of 4.4 gauss. An explanation of this narrowing may lie in the linking of water molecules to each other, which is likely when the number of water molecules of hydration is large.[13] If such ice-like substructures are, for some reason, prevalent in borax, we may expect that the protons of these substructures are moving back and forth between oxygens in a double-minimum potential well, a model successfully applied by Pauling in calculating the residual entropy of ice.[14] Reorientations in ice are indicated both by dielectric dispersion[15] and by thermal relaxation in nuclear resonance experiments.[16] Motion or shuttling of this type leads, in general, to reduced line widths[1,16,17] and invalidates the assumption, made in explaining fine structure, that the nuclei are rigidly fixed.

Some experimental evidence exists bearing on this question. No fine structure is reported in

[11] See reference 5, p. 368.

[12] See a forthcoming paper by J. H. Van Vleck.

[13] See reference 5, Chapter XI, especially p. 369.

[14] See reference 10, p. 303.

[15] Debye, *Polar Molecules* (Dover Publications, Inc., 1945), Chapter V.

[16] N. Bloembergen, E. M. Purcell, and R. V. Pound, Nature 160, 475 (1947). Line width in this reference is approximately twice that we have defined.

[17] C. J. Gorter and J. H. Van Vleck, Phys. Rev. 72, 1128 (1947).

ice, and the line width at $-5°C$ is about 2.5 gauss,[16] although it increases at lower temperatures. Pitzer and Coulter[18] report approximately 2/10 as much residual entropy per H_2O molecule in $Na_2SO_4 \cdot 10H_2O$ as exists in ice; a tendency toward smoothed-out fine structure in this substance is mentioned in Section 4. If this explanation of the narrower line is correct, the residual entropy per H_2O molecule of borax should approach that of ice. So far as the author knows, this quantity has not yet been determined.

On the basis of these preliminary experiments, the study of nuclear resonance absorption fine structure appears to hold some promise toward extending knowledge not only of the solid state, but also of the role of hydrogen in chemical bonding. Investigations of the latter have been especially hampered by the inability of x-ray methods to locate hydrogen atoms. The method, if it is applicable to the substance in question, is favorable for the determination of internuclear distances, inasmuch as the directly measured quantity is the cube of the distance. Thus, although magnetic field calibration, finite modulation, noise fluctuations, and crudeness of crystal cutting may have introduced as much as 6 percent error in the determination of r^3, the value of r should not be in error by more than 2 percent.

[18] K. S. Pitzer and L. V. Coulter, J. Am. Chem. Soc. 60, 1310 (1938).

ACKNOWLEDGMENT

The author wishes to thank Professor E. M. Purcell, under whom this work was carried out, for his expert guidance and helpful advice. It is a pleasure to acknowledge many instructive discussions with R. V. Pound and N. Bloembergen. Facilities for the experimental work reported, including the large permanent magnet, were provided through a Frederick Gardner Cottrell Special Grant-in-Aid from the Research Corporation.

THE JOURNAL OF CHEMICAL PHYSICS VOLUME 16, NUMBER 4 APRIL, 1948

The Conductance of Sodium and Potassium Chlorides in 50-Mole Percent Methanol-Water Mixtures

H. I. SCHIFF AND A. R. GORDON
Chemistry Department, University of Toronto, Toronto, Canada

(Received December 10, 1947)

The conductance of NaCl and KCl in 50-mole percent methanol-water mixtures has been measured at concentrations from 0.0005 to 0.01 *N*. The data can be represented within experimental error by the Onsager-Shedlovsky equation, the limiting conductances being 66.62 and 75.10, respectively. The limiting conductances of chloride ion, obtained from these values, and the limiting transference numbers reported in the accompanying paper, satisfy the rule of independent ionic mobilities, but at finite concentrations the chloride ion conductance is less for the potassium salt than for the sodium. The decrease in limiting ion conductances as compared with those in water is greater than can be accounted for by viscosity alone. The results are also in disagreement with the Bjerrum theory of ion pair formation if the mean ionic diameter, determined thermodynamically, is significant in transport processes.

THE work reported here was undertaken to provide values of the conductance for two typical 1-1 electrolytes in 50-mole percent methanol-water solution, and so make possible a correlation of the transference data[1] given in the accompanying paper.

The procedure employed was the same as that used in this laboratory for aqueous solutions, *viz.* the direct current method with reversible Ag/AgCl probe electrodes as described by Gunning and Gordon;[2] for details of cell, circuit,

[1] L. W. Shemilt, J. A. Davies, and A. R. Gordon, J. Chem. Phys. 16, 340 (1948).

[2] H. E. Gunning and A. R. Gordon, J. Chem. Phys. 10, 126 (1942); *ibid.* 11, 18 (1943); G. C. Benson and A. R. Gordon, J. Chem. Phys. 13, 470 (1945); *ibid.* 13, 473 (1945).